A New United Atom Force Field for Adsorption of Alkenes in Zeolites

Bei Liu,*,† Berend Smit,†,‡ Fernando Rey,§ Susana Valencia,§ and Sofía Calero⊥

Van't Hoff Institute for Molecular Sciences, University of Amsterdam, Nieuwe Achtergracht 166, 1018 WV Amsterdam, The Netherlands, Centre Européen de Calcul Atomique et Moléculaire (CECAM), Ecole Normale Supérieure, 46 allée d'Italie, 69007 Lyon, France, Instituto de Tecnología Química (UPV-CSIC), Avda. de los Naranjos s/n. 46022 Valencia, Spain, and Department of Physical, Chemical, and Natural Systems, University Pablo de Olavide, Ctra. Utrera km. 1. 41013 Seville, Spain

Received: July 24, 2007; In Final Form: September 25, 2007

A new united atom force field was developed that accurately describes the adsorption properties of linear alkenes in zeolites. The force field was specifically designed for use in the inhomogeneous system and therefore a truncated and shifted potential was used. With the determined force field, we performed a comparative study on the adsorption behaviors of ethene and propene in four pure-silica small-pore eight-membered-ring zeolites, CHA, DDR, ITE, and IHW (named Chabazite, DD3R, ITQ-3, and ITQ-32, respectively), characterized for their paraffin/olefin separation capability. The different macroscopic adsorption behaviors of alkenes in the four zeolites were elucidated and related to their structures with the microscopic information obtained from the molecular simulations providing useful information for further rational design of such zeolites with tailored properties.

1. Introduction

In recent years there has been considerable interest in separation technology concerning olefin/paraffin systems. Many microporous materials such as zeolites are recognized as promising candidates for this purpose based on their adsorption and diffusion properties.[1−12] Therefore, it is important to explore the adsorption and diffusion behaviors of hydrocarbons in different zeolites. In addition to experiment, molecular simulation has proved to be a useful tool to investigate the properties of fluids confined in porous materials.[13] Although there are numerous simulation studies on the adsorption and diffusion of alkanes in zeolites, theoretical studies concerning the alkenes in zeolites are scarce,[2,14−18] mainly due to the absence of suitable force fields.

Many united-atom (UA) force fields[19−23] have been proposed recently that can accurately and quantitatively describe the adsorption and diffusion properties of alkanes in nanoporous framework structures. However, to the best of our knowledge, there are only two UA force fields dealing with the adsorption of alkenes in zeolites.[14,18] The first one was developed by Jakobtorweihen et al.[14] This force field accurately describes the adsorption properties of alkenes in the Silicalite (MFI) zeolite as well as in the Theta-1 (TON) and DD3R (DDR) zeolites. This force field, however, uses tail corrections which make it less practical to use in inhomogeneous systems.[24,25] The other one is the extended version of this force field to include the effects of sodium cations by Granato et al.[18] As most of the accurate alkane models do not use these tail corrections for doing proper adsorption and diffusion in this type of systems, it is important to have a similar type of model for both alkanes and alkenes.

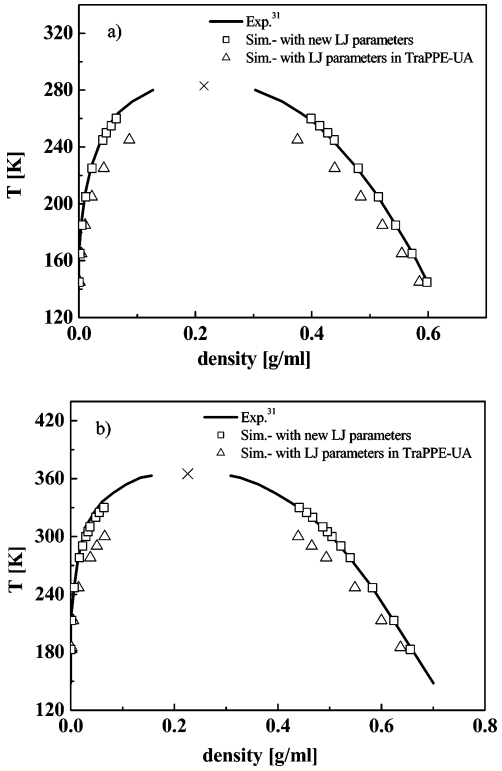

Figure 1. Vapor−liquid coexistence curves for (a) ethene and (b) propene.

Pure silica small-pore eight-membered-ring (8R) zeolites have been recognized as promising candidates for olefin/paraffin separation.[1−4] Although various pure silica 8R zeolites have been experimentally characterized for their alkene adsorption and olefin/paraffin separation capability,[1−4,8,15,26] theoretical studies concerning the diffusion and adsorption of alkenes in these kinds of zeolites are very scarce.[2,15,16] The only available work is that of ter Horst et al.,[16] who studied the diffusion of propene in the

* Corresponding author. E-mail: bliu@science.uva.nl.
† University of Amsterdam.
‡ Ecole Normale Supérieure.
§ Instituto de Tecnología Química.
⊥ University Pablo de Olavide.

10.1021/jp075809d CCC: $40.75 © 2008 American Chemical Society
Published on Web 01/25/2008

TABLE 1. Force Field Parameters Used in This Work[a]

	O		$CH_3(sp^3)$		$CH_2(sp^3)$		$CH_2(sp^2)$		$CH(sp^2)$	
	σ_{ij}	ϵ_{ij}/k_B	σ_{ij}	ϵ_{ij}/k_B	σ_{ij}	ϵ_{ij}/k_B	σ_{ij}	ϵ_{ij}/k_B	σ_{ij}	ϵ_{ij}/k_B
$CH_3(sp^3)$	3.48	93	3.76	108	3.86	77.77	3.72	100.22	3.75	75.66
$CH_2(sp^3)$	3.58	60.5	3.86	77.77	3.96	56	3.82	72.17	3.85	54.48
$CH_2(sp^2)$	***3.53***	***82.05***	3.72	100.22	3.82	72.17	***3.685***	***93***	3.71	70.21
$CH(sp^2)$	***3.502***	***55.215***	3.75	75.66	3.85	54.48	3.71	70.21	***3.74***	***53***

bond lengths	r_0 (Å)
CH_i-CH_j	1.54
$CH_i=CH_j$	1.33

bend: $U^{bend} = {}^1/_2 k_0(\theta - \theta_0)^2$; $k_0/k_B = 70400$ K; $\theta_0 = 119.70°$

torsion: $U_{torsion} = c_0 + c_1[1 + \cos(\phi)] + c_2[1 - \cos(2\phi)] + c_3[1 + \cos(3\phi)]$

c_n/k_B in K	c_0	c_1	c_2	c_3
	688.5	86.36	−109.77	−282.24

[a] LJ parameters σ_{ij} in Å and ϵ_{ij}/k_B in K. The $CH_i(sp^3)-CH_i(sp^3)$ and $CH_i(sp^3)$−oxygen interaction parameters were taken from ref 19 and the internal bond, bend, and torsion parameters were taken from ref 30. The parameters proposed in this work are given as bold italics.

pure-silica zeolite DD3R with the commercial program package Cerius2, and the very crude simulations on the adsorption of alkenes in the zeolites DD3R and ITQ-12 with Cerius2 as a support for the experimental measurements.[2,15] At present there are much more accurate force fields available compared to the ones in Cerius2. Considering that there are eleven 8R zeolites that can be prepared as pure silica and their potential application for olefin separation, it is worth performing a systematic comparative study for some of them, for which molecular simulation is the most suitable tool. Therefore, with the newly developed force field, this work performed a systematic molecular simulation study on the adsorption of ethene and propene in four pure-silica 8R zeolites with different pore topologies, Chabazite (CHA), DD3R (DDR), ITQ-3 (ITE), and ITQ-32 (IHW). The microscopic information obtained from the molecular simulations was used to elucidate the different macroscopic adsorption behavior of the four zeolites to provide useful information for further rational use of such zeolites.

2. Simulation Technique

To test the accuracy of the alkene−alkene interactions, the vapor−liquid coexistence curves (VLCC) were computed by using the *NVT* version of Gibbs ensemble.[27,28] For the calculation of Henry coefficient and the isosteric heats of adsorption at infinite dilution Q_{st}^0, we performed configurational-bias Monte Carlo (CBMC) simulations in the *NVT* ensemble. During the simulation we computed the Rosenbluth factor and the internal energy ΔU, which are directly related to the Henry coefficient and Q_{st}^0, respectively.[20,29] Adsorption isotherms were calculated in the grand-canonical ensemble with use of the CBMC method. A detailed description of the simulation methods can be found in ref 20.

3. Results and Discussion

3.1. Development of the New UA Force Field. In the present work, the united atom model was used, in which $CH_3(sp^3)$, $CH_2(sp^2)$, and $CH(sp^2)$ groups are considered as a single pseudoatom or united atom. The Lennard-Jones 12−6 potential was used, which is truncated at a cutoff (r_{cut}) of 12 Å and shifted so that the energy tends smoothly to zero at the cutoff.

3.1.1. Alkene−Alkene Interaction. The TraPPE-UA force field for alkenes[30] was used in this work. The bond length between the atoms was kept fixed. Harmonic potential models the bond bending between three neighboring beads, and the torsion potential used in the TraPPE-UA force field[30] was adopted in this work controlling the torsional angle. The effective Lennard-Jones (LJ) interaction parameters for the $CH_i(sp^3)$ groups were taken from the ref 19 and the ones between the $CH_2(sp^2)-CH_2(sp^2)$ and $CH(sp^2)-CH(sp^2)$ groups were optimized in this work to reproduce the vapor−liquid coexistence curves for ethene and propene. The experimental curves[31] and our simulation results based on the TraPPE-UA (using the truncated and shifted potential instead of the truncated potential with tail corrections) as well as on the new LJ parameters (all the parameters are listed in Table 1) are shown in Figure 1a,b. Obviously, the coexistence densities were well reproduced by our new parameters, much better than that from the original TraPPE-UA parameters.

3.1.2. Alkane−Zeolite Interaction. To keep the consistency of all interaction parameters used in this work we adopted the united atom force field proposed by Dubbeldam et al.[19] for describing the interactions between $CH_i(sp^3)$ centers and the oxygen atoms of the zeolite framework. This force field faithfully reproduces the experimentally determined isotherms (particularly the inflection points) in pure silica MFI-type zeolites and has been successfully extended to most types of pure silica zeolites.[20,32,33]

3.1.3. Alkene−Zeolite Interaction. Following a similar strategy as employed in our previous work[19−23] for the development of the UA force field for alkane−zeolite systems, simulations were performed first for the adsorption isotherms of ethene, propene, and 1-butene to determine the effective LJ interaction parameters for the $CH_2(sp^2)$, $CH(sp^2)$, and the oxygen atoms of the zeolite framework. Ideally, one would like to calibrate a force field on various data sets from different authors. Therefore the experimental values measured in MFI zeolites were adopted here as the calibration set. Our simulation results as well as the experimental[34−41] and previous simulation results[14,17] are shown in Figure 2a−c. We found that our UA force field faithfully reproduces the experimental isotherms and shows comparable results with previous simulations. It should be pointed out that in Jakobtorweihen et al.'s work[14] the tail correction was used, while in Pascual et al.'s work[17] a more complex anisotropic united atom (AUA) potential scheme was used.

Having obtained the parameters for $CH_2(sp^2)-O$ and $CH(sp^2)-O$, we need to check their validity. First, the isosteric

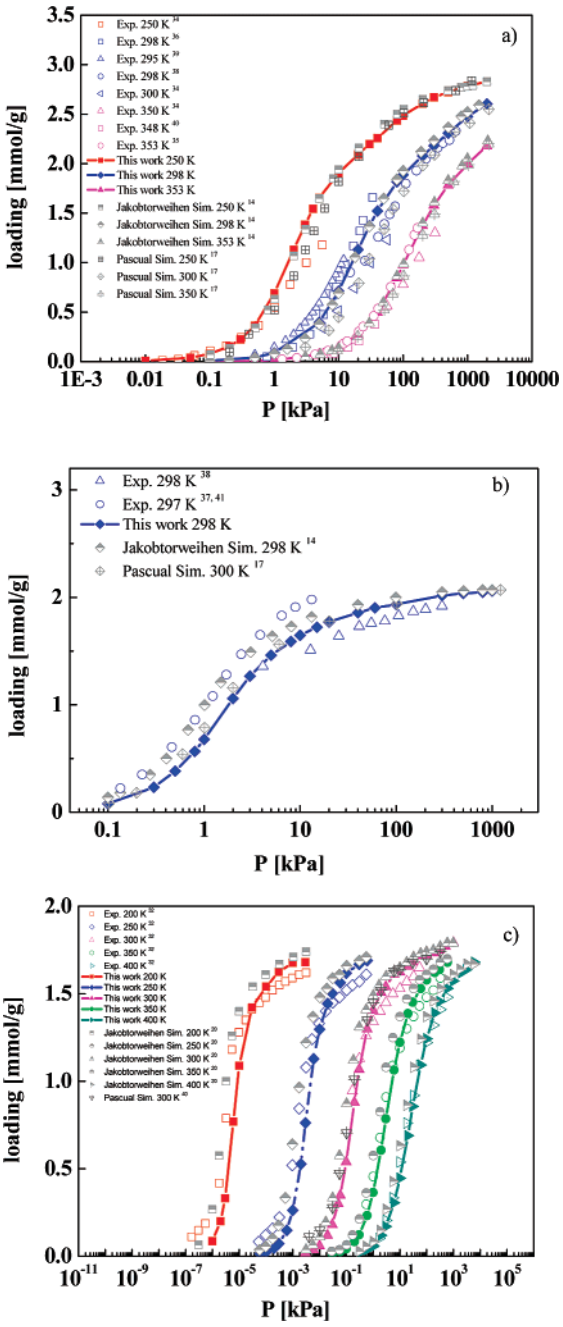

Figure 2. Comparison of the experimental and simulated adsorption isotherms of (a) ethene, (b) propene, and (c) 1-butene in MFI zeolites.

heats of adsorption at infinite dilution Q_{st}^0 for ethene, propene, and 1-butene in MFI zeolite were calculated, as shown in Table 2. The calculated results based on our new force field show comparable results with Jakobtorweihen et al.'s simulations and are in the range of the experimental data, closing to the mean value between the lowest and the highest experimental values.

TABLE 2. Isosteric Heats of Adsorption at Infinite Dilution Q_{st}^0 [kJ/mol] of Alkenes in MFI Zeolite at 298 K

	ethene	propene	1-butene
exptl data[a]	24.0−32.7	40.0	46.0−51.5
this work	28.2	38.1	46.6
Jakobtorweihen et al.[14]	27.6	38.3	46.4

[a] The experimental data are taken from Table 3 in ref 14.

TABLE 3. Henry Coefficients K_H and Isosteric Heats of Adsorption at Infinite Dilution Q_{st}^0 of Propene at 303 K

	K_H (mol/kg/Pa)		Q_{st}^0 (kJ/mol)	
zeolite	sim.	exptl[2,45]	sim.	exptl
DD3R	9.67×10^{-4}	7.54×10^{-4}	35.6	36.0[2]
CHA	5.28×10^{-4}		33.0	33.5[3]
ITQ-3	4.52×10^{-4}		31.6	28.5[3]
ITQ-32	7.25×10^{-4}	11.61×10^{-4}	36.0	33.6[45]
TON	4.24×10^{-4}		39.8	

To demonstrate that our parameters are transferable to other pure silica zeolites other than MFI, we also calculated the adsorption isotherms, together with those of Henry coefficients and isosteric heat of adsorption at infinite dilution of ethene and propene in TON, DD3R, ITQ-29, CHA, ITQ-3, and ITQ-32 zeolites and compared with experimental data available,[2,3,42−45] as shown in Table 3 and Figures 3 and 4.

Figure 3 shows for ethene the agreement between our simulations and the experiments is good for TON, ITQ-29 (our simulations agree well with the experimental data of ref 43 at 298 K, but less with that of ref 44 at 301 K, attributing to the existence of discrepancy between experimental data measured by different authors), and CHA, but less for DD3R. For the latter, our simulations show systematically higher values than the experimental observations and similar deviation has been observed by other simulations with use of a different force field.[14] The discrepancy between simulations and experiments may be attributed to the perfect structures used in the simulations, while the experimental samples may be not completely accessible due to intergrowths and partial blocking of the pores. Also this discrepancy can be related to the large diffusional limitations due to the very large crystal size that generally is observed in pure silica zeolites, precluding reaching thermodynamic equilibrium in the experimental data.

For propene, as a first step the Henry coefficients and the isosteric heat of adsorption at infinite dilution Q_{st}^0 were calculated, and compared with experimental values[2,3,45] whenever available, as shown in Table 3. Again the discrepancy between simulations and experiments may be attributed to the reasons that simulations are always assuming perfect and infinite crystals as well as equilibrium. However, experimentally this is not the case and generally crystals are far from being perfect. Of course, the amount of defects will depend on the thermal history, synthesis method, etc. used to prepare the sample. Then, this

TABLE 4. Structural Information for the Four Pure Silica 8R Zeolites Used in This Work

			simulation cell size (Å)			
zeolite	topology	unit cell	*x*	*y*	*z*	ring size (Å)
DD3R [52]	2-d	$a = 13.860$, $c = 40.89$ Å trigonal ($R\bar{3}m$)	41.58	41.58	40.89	3.7 × 4.4
CHA [47]	3-d	$a = 13.529$, $c = 14.748$ Å trigonal ($R\bar{3}m$)	27.058	27.058	29.496	3.8 × 3.8
ITQ-3 [53]	1-d	$a = 20.622$, $b = 9.724$, $c = 19.623$ Å orthorhombic (*Cmcm*)	41.244	38.896	39.246	3.8 × 4.3
ITQ-32 [26]	2-d	$a = 13.699$, $b = 24.067$, $c = 18.197$ Å orthorhombic (*Cmca*)	27.398	48.134	36.394	3.5 × 4.3

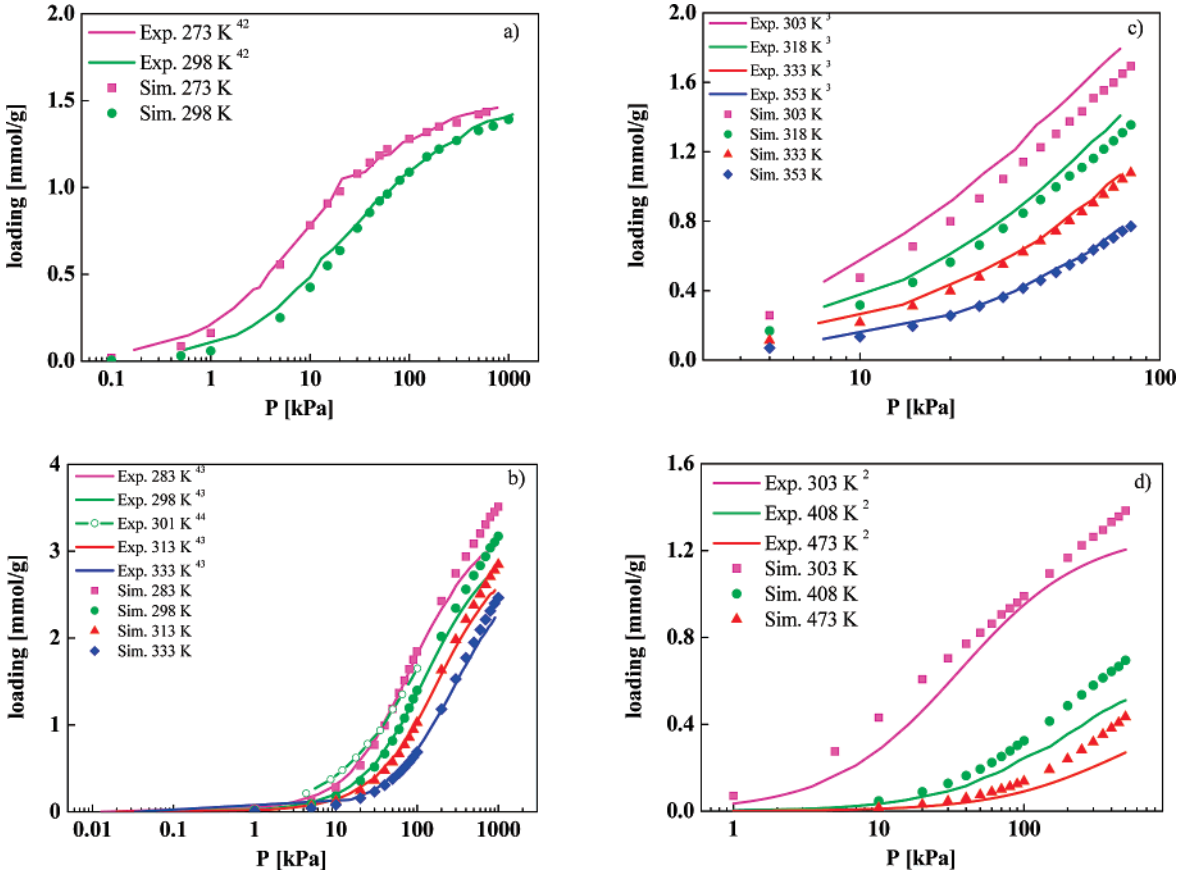

Figure 3. Comparison of the experimental and simulated adsorption isotherms of ethene in (a) TON, (b) ITQ-29, (c) CHA, and (d) DD3R zeolites.

cannot be accounted for in theoretical studies. A second source (and at least equally important) is the accuracy of experimental methods and the corresponding adsorption models used during the data analysis for calculating the Henry coefficients and heats of adsorption. For instance, the experimental data on the pure silica ITQ-32 sample were obtained by some of the authors of this paper and published in ref 45 as Supporting Information. In this work, these data were fitted using the Virial formalism to describe the isotherm and the Henry coefficients were calculated at each temperature (25, 60, and 90 °C). The Heats of adsorption were calculated by using the Clausius-Clapeyron equation. Our experimental error for the heat of adsorption is larger than 3 kJ/mol and therefore there is a good agreement between experimental and calculated results. On the other hand, since the uncertainty of the K_H values in this case is much higher than that in Q_{st} values, the differences in order of magnitude are meaningful. Furthermore, the adsorption isotherms of propene were computed and given in Figure 4, showing that the experimental isotherms could be accurately predicted for ITQ-3 and ITQ-32 zeolites. For DD3R, a similar behavior as ethene was found, that is, simulated uptakes are higher than the experimental data. Again, this may be attributed to the fact that diffusional restrictions are limiting to fully reach equilibrium in the experimental measurements or to the presence of some low-porous amorphous silica which could accompany the DD3R sample studied in ref 2. CHA is another case in which our simulations show systematically lower values than the experimental observations. The reason might be the sensitivity of the Lennard-Jones potential for small changes in the parameters when the oxygen and carbon groups are in close proximity.[46] This effect would be enlarged when the adsorbate is bigger.

The simulation results of the adsorption isotherms, together with those of the Henry coefficients and the isosteric heat of adsorption at infinite dilution, show that the UA force field proposed in this work is applicable to most pure silica zeolites and can be used for the characterization of alkene adsorption in the zeolites.

3.2. Comparison of Alkene Adsorption in Pure-Silica CHA, DD3R, ITQ-3, and ITQ-32 Zeolites. With the determined force field, we further performed a molecular simulation study on the adsorption of alkenes in four typical pure silica 8R zeolites with different pore topologies, CHA, DD3R, ITQ-3, and ITQ-32, since they have been recognized as promising candidates for the separation of alkene from olefin/paraffin mixtures in the petrochemical industry.[1−4,45]

3.2.1. Zeolite Models. The structures of DD3R, CHA, and ITQ-3 are well-known and have been used in many previous simulation studies.[14,16,20,48−51] The DDR-type zeolite consists of 19-hedron cavities connected through 8R windows across a hexagonally arranged two-dimensional cage/window-type system. The CHA-type zeolite consists of an ellipsoidal cavity through 0.38 nm wide 8R windows. ITQ-3 has a one-dimensional pore system with small windows of about 0.4 nm in diameter made up of 8R that open to larger cavities. A second straight channel runs through the material but is too narrow to accommodate guest molecules. ITQ-32 has been synthesized recently[26] and has never been the focus of a simulation. It exhibits a unidirectional small 8R channel system along the *x*-axis, with a pore aperture of 3.5 × 4.3 Å, which is crossed perpendicularly by relatively short 12R channels. The 12R channels interconnect two neighbored 8R channels along the *z* direction, resulting in a bidirectional pore structure. The structures of the four zeolites are shown in Figure 5, and some details of the structures of the four zeolites are summarized in Table 4. In the simulations, the zeolite structures were constructed by using the atomic coordinates reported,[26,47,52,53] and

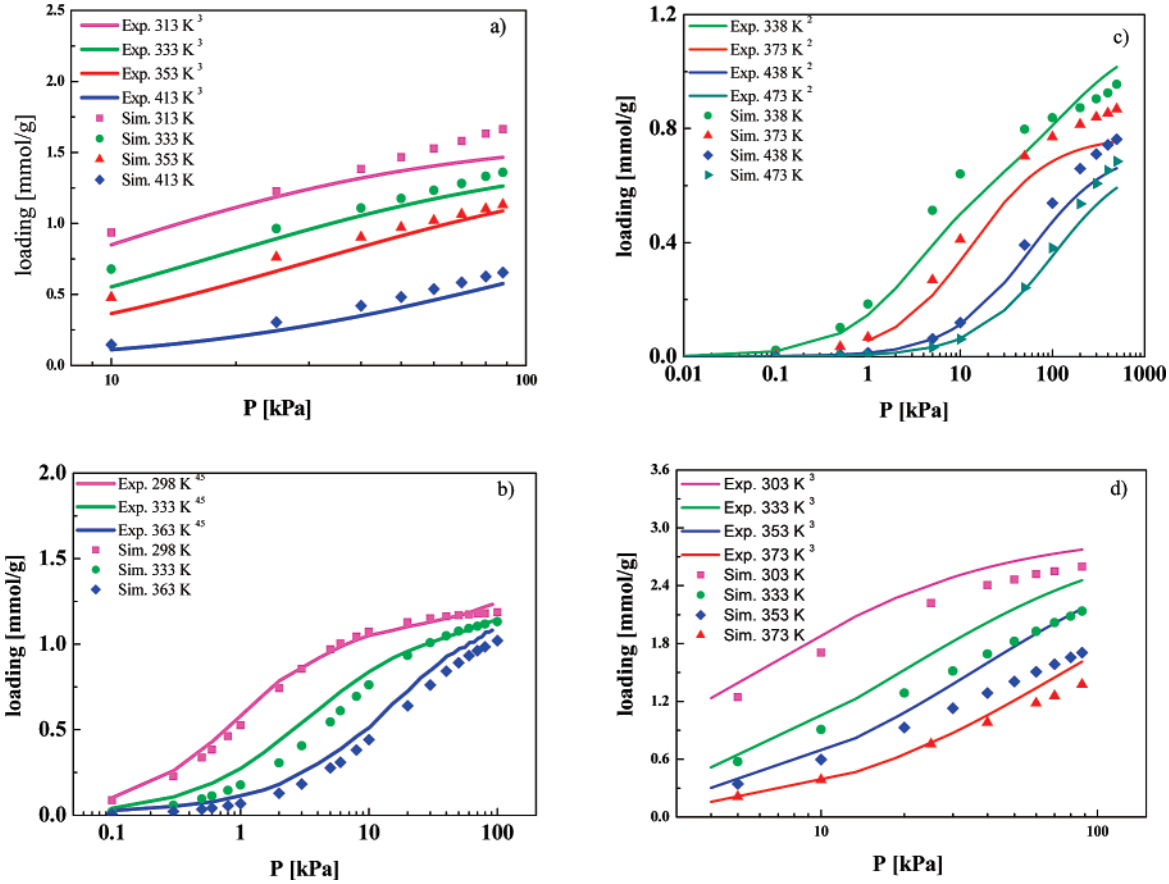

Figure 4. Comparison of the experimental and simulated adsorption isotherms of propene in (a) ITQ-3, (b) ITQ-32, (c) DD3R, and (d) CHA zeolites.

the zeolite lattices were assumed to be rigid in the simulations since the flexibility of the framework has a negligible influence on the adsorption properties.[54]

3.2.2. Comparison of Alkene Adsorption Behaviors. To compare the adsorption behaviors of alkenes in the four typical 8R zeolites, DD3R, CHA, ITQ-3, and ITQ-32, the adsorption isotherms of ethene and propene in them at 303 K were simulated, as shown in Figure 6a,b.

For ethene at low pressures, the order of the adsorption capacity is DD3R > ITQ-32 > CHA > ITQ-3; at high pressures, the order changed to CHA > ITQ-3 > DD3R ≈ ITQ-32. This agrees with the order of the experimentally measured void volumes of the four zeolites determined by N_2 adsorption measurements: CHA, 0.3 cm^3/g;[47] ITQ-3, 0.23 cm^3/g;[47] ITQ-32, 0.16 cm^3/g;[26] and DD3R, 0.15 cm^3/g.[2] The order of the propene adsorption capacity is the same as the one for ethene at low pressures, agreeing well with the order of the experimental Q_{st}^0 presented in Table 3, while at high pressures, the order changed to ITQ-3 > CHA > ITQ-32 ≈ DD3R. The adsorption capacity of a zeolite is affected by various factors, and the main ones are surface area, the interactions between adsorbate and adsorbent, packing of adsorbate molecules inside the void spaces of the adsorbent, and the available void volumes. At very low pressures (close to infinite dilution), the interactions between adsorbate and adsorbent are a predominant factor, while at sufficient high pressures it is determined by the effective void volume. The adsorption behavior is the result of the cooperative effects of the various factors. This explains the changes of the adsorption capacities with pressures of the four zeolites shown in Figure 6a,b.

In addition to the differences in adsorption capacities, the shapes of the adsorption isotherms are also different for the four zeolites. The inflection behavior was found on the adsorption isotherm for DD3R at a loading of 12 molecules per unit cell for ethene and 6 for propene. This corresponds to 2 molecules per accessible cage for ethene and 1 for propene since one unit cell of DD3R has six 19-hedron cages.[2] In view of the free volume, the 19-hedron cavity is large enough for 2 ethene molecules, but also allows the adsorption of exactly two propene molecules, which is possible only in a certain arrangement. If all the cages are filled with one molecule, insertion of an additional molecule requires some energy for the rearrangement. Consequently, a second inflection behavior occurs evidently at higher pressures, for a loading of 2 propene molecules per accessible cage. In the case of ITQ-32, similar adsorption behavior as DDR is observed, that is, the inflection behavior occurs at a loading of 12 molecules per unit cell for ethene, and 6 for propene were observed. The underlying mechanism is the same as that for DD3R. As for CHA, the inflection behavior was found at a loading of 6 molecules per unit cell for ethene and no inflection occurred for propene. A unit cell of CHA contains a single cage with 6 eight-membered 0.38 nm wide ring windows. The guest molecules have to pass through the windows to enter the cage. The cage can host more than 6 ethene molecules (but much more energy is needed for insertion after 6 molecules per cage) and exactly 6 propene molecules. ITQ-3, on the other hand, has four cavities per unit cell. The adsorption isotherms do not show any obvious inflection and the maximum capacity for ethene is 4 molecules/cavity and 3 molecules/cavity for propene.

4. Conclusions

The UA force field developed in this work can accurately describe the adsorption properties of linear alkenes in several

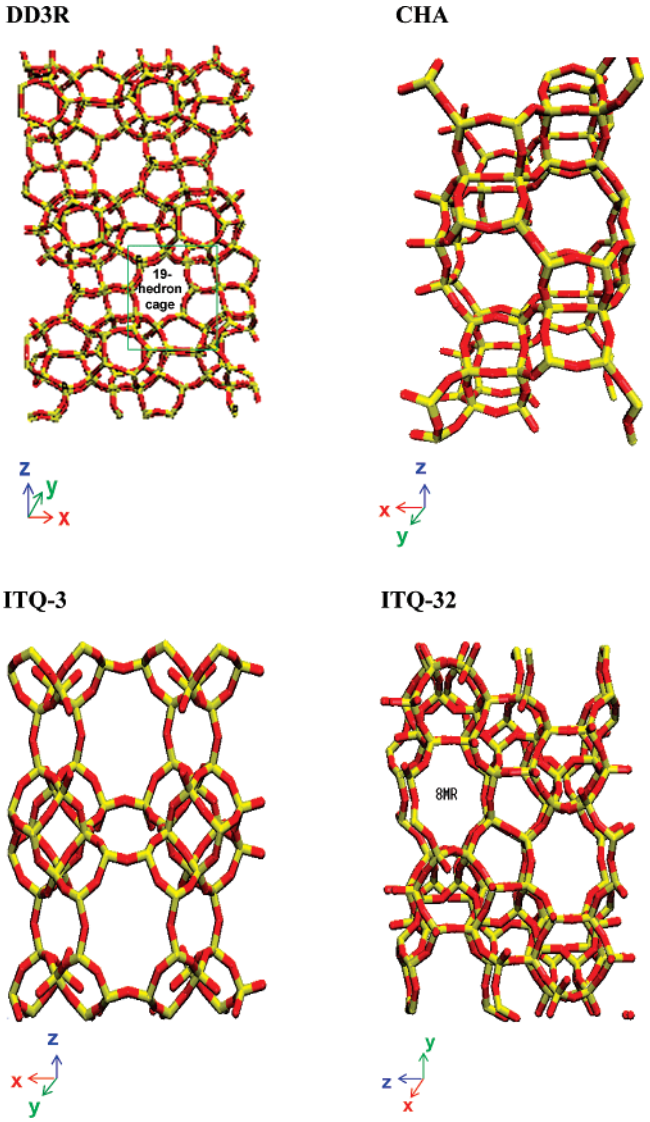

Figure 5. The structures of DD3R, CHA, ITQ-3, and ITQ-32.

pure silica zeolites, such as MFI, TON, ITQ-29, ITQ-3, ITQ-32, CHA, and DD3R. The results show that it is a general force field applicable to most pure silica zeolites.

On the basis of this new force field, the different macroscopic alkene adsorption behaviors of the four 8R zeolites, CHA, DD3R, ITQ-3, and ITQ-32, were elucidated with the microscopic information obtained from the molecular simulations, and a systematic comparison was made by relating their adsorption behavior to their structures.

Finally, it should be pointed out that, compared with the available UA force field of Jakobtorweihen et al., the new force field does not include tail corrections, and thus can be used to simulate the diffusion of alkenes in zeolites. The study on this topic is ongoing and the results will be presented in our future work.

Acknowledgment. This work is supported by the Dutch STW/CW Separation Technology program (700.56.655-DPC.6243) and the EC through Marie Curie EXT project MEXT-CT-2005-023311, by the Spanish "Ministerio de Educación y Ciencia" (CTQ2007-63229/BQU), and by the resources, technical expertise, and assistance provided by BSC-CNS. F.R. and S.V. acknowledge Spanish MEC projects MAT2006-08039 and CTQ2004-02510/PPQ for financial support. The authors wish to thank E. Beerdsen and A. V. Gaikwad for useful discussions.

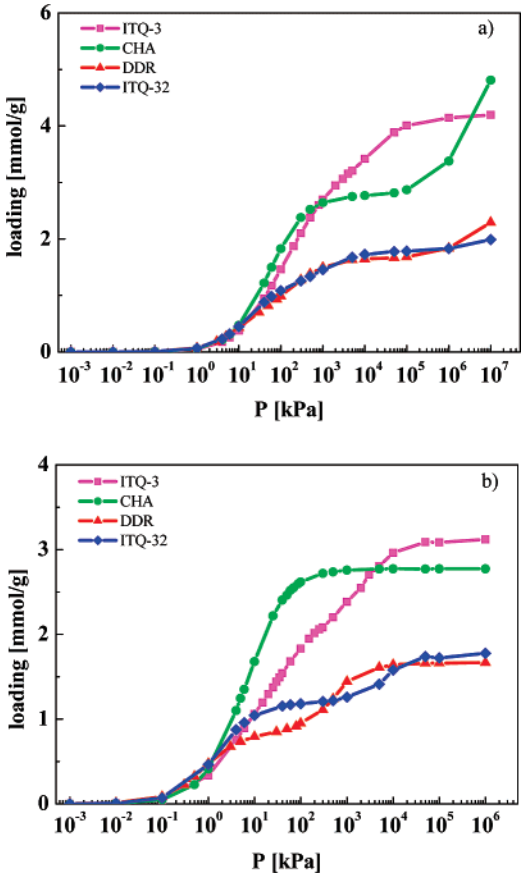

Figure 6. Simulated adsorption isotherms of (a) ethene and (b) propene in DD3R, CHA, ITQ-3, and ITQ-32 zeolites at 303 K.

References and Notes

(1) Zhu, W.; Kapteijn, F.; Moulijn, J. A. *Chem. Commun.* **1999**, 2453.
(2) Zhu, W.; Kapteijn, F.; Moulijn, J. A.; den Exter, M. C.; Jansen, J. C. *Langmuir* **2000**, *16*, 3322.
(3) Olson, D. H.; Camblor, M. A.; Villaescusa, L. A.; Kuehl, G. H. *Microporous Mesoporous Mater.* **2004**, *67*, 27.
(4) Olson, D. H. U.S. Patent 6,488,741, 2002.
(5) Kantner, E.; Savage, D. W.; Bellows, R. J. U.S. Patent 5,292,990, 1994.
(6) Kulprathipanja, S. U.S. Patent 4,433,195, 1984.
(7) Daems, I.; Leflaive, P.; Methivier, A.; Denayer, J. F. M.; Baron, G. V. *Microporous Mesoporous Mater.* **2005**, *82*, 191.
(8) Olson, D. H.; Yang, X.; Camblor, M. A. *J. Phys. Chem. B* **2004**, *108*, 11044.
(9) Grande, C. A.; Gigola, C.; Rodrigues, A. E. *Adsorption* **2003**, *9*, 321.
(10) Da Silva, F. A.; Rodrigues, A. E. *Ind. Eng. Chem. Res.* **1999**, *38*, 2434.
(11) Jarvelin, H.; Fair, J. R. *Ind. Eng. Chem. Res.* **1993**, *32*, 2201.
(12) Rege, S. U.; Padin, J.; Yang, R. T. *AIChE J.* **1998**, *44*, 799.
(13) Catlow, C. R. A.; van Santen, R. A.; Smit, B. *Computer Modelling of Microporous Materials*; Elsevier Science: Amsterdam, The Netherlands, 2004.
(14) Jakobtorweihen, S.; Hansen, N.; Keil, F. J. *Mol. Phys.* **2005**, *103*, 471.
(15) Yang, X.; Toby, B. H.; Camblor, M. A.; Lee, Y.; Olson, D. H. *J. Phys. Chem. B* **2005**, *109*, 7894.
(16) ter Horst, J. H.; Bromley, S. T.; van Rosmalen, G. M.; Jansen, J. C. *Microporous Mesoporous Mater.* **2002**, *53*, 45.
(17) Pascual, P.; Ungerer, P.; Tavitian, B.; Boutin, A. *J. Phys. Chem. B* **2004**, *108*, 393.
(18) Granato, M. A.; Vlugt, T. J. H.; Rodrigues, A. E. *Ind. Eng. Chem. Res.* **2007**, *46*, 321.
(19) Dubbeldam, D.; Calero, S.; Vlugt, T. J. H.; Krishna, R.; Maesen, T. L. M.; Beerdsen, E.; Smit, B. *Phys. Rev. Lett.* **2004**, *93*, 088302.

(20) Dubbeldam, D.; Calero, S.; Vlugt, T. J. H.; Krishna, R.; Maesen, T. L. M.; Smit, B. *J. Phys. Chem. B* **2004**, *108*, 12301.
(21) Calero, S.; Dubbeldam, D.; Krishna, R.; Smit, B.; Vlugt, T. J. H.; Denayer, J. F. M.; Martens, J. A.; Maesen, T. L. M. *J. Am. Chem. Soc.* **2004**, *126*, 11377.
(22) Calero, S.; Lobato, M. D.; García-Pérez, E.; Mejías, J. A.; Lago, S.; Vlugt, T. J. H.; Maesen, T. L. M.; Smit, B.; Dubbeldam, D. *J. Phys. Chem. B* **2006**, *110*, 5838.
(23) García-Pérez, E.; Dubbeldam, D.; Maesen, T. L. M.; Calero, S. *J. Phys. Chem. B* **2006**, *110*, 23968.
(24) Martin, M. G.; Thompson, A. P.; Nenoff, T. M. *J. Chem. Phys.* **2001**, *114*, 7174.
(25) Wilding, N. B.; Schoen, M. *Phys. Rev. E* **1999**, *60*, 1081.
(26) Cantín, A.; Corma, A.; Leiva, S.; Rey, F.; Rius, J.; Valencia, S. *J. Am. Chem. Soc.* **2005**, *127*, 11560.
(27) Panagiotopoulos, A. Z. *Mol. Phys.* **1987**, *61*, 813.
(28) Panagiotopoulos, A. Z.; Quirke, N.; Stapleton, M.; Tildesley, D. J. *Mol. Phys.* **1988**, *63*, 527.
(29) Frenkel, D.; Smit, B. *Understanding Molecular Simulations*: *From Algorithms to Applications*, 2nd ed.; Academic Press: San Diego, CA, 2002.
(30) Wick, C. D.; Martin, M. G.; Siepmann, J. I. *J. Phys. Chem. B* **2000**, *104*, 8008.
(31) Smith B. D.; Srivastava, R. *Thermodynamic Data for Pure Compounds*: *Part A*, *Hydrocarbons and Ketones*; Elsevier: Amsterdam, The Netherlands, 1986.
(32) Liu, B.; Smit, B.; Calero, S. *J. Phys. Chem. B* **2006**, *110*, 20166.
(33) Chong, S. S.; Jobic, H.; Plazanet, M. *Chem. Phys. Lett.* **2005**, *408*, 157.
(34) Stach, H.; Lohse, U.; Thamm, H.; Schirmer, W. *Zeolites* **1986**, *6*, 74.
(35) Choudhary, V. R.; Mayadevi, S. *Zeolites* **1996**, *17*, 501.
(36) Hampson, J. A.; Rees, L. V. C. Fundamentals of Adsorption. In *Studies in Surface Science and Catalysis*; Suzuki, M., Ed.; Kodansha/Elsevier: Tokoy/Amserdam, 1993; pp 259−266.
(37) Jen, H. W.; Otto, K. *Catal. Lett.* **1994**, *26*, 217.
(38) Hampson, J. A.; Jasra, R. V.; Rees, L. V. C. Characterization of porous Solids II. In *Studies in Surface Science and Catalysis*; Rodriguez-Reinoso, F., Rouquerol, J., Sing, K. S. W., Unger, K. K., Eds.; Elsevier: Amserdam, The Netherlands, 1991; pp 509−517.
(39) Bakker, W. J. W.; Kapteijn, F.; Poppe, J.; Moulijn, J. A. *J. Membr. Sci.* **1996**, *117*, 57.
(40) Gladden, L. F.; Hargreaves, M.; Alexander, P. *Chem. Eng. J.* **1999**, *74*, 57.
(41) Otto, K.; Montreuil, C. N.; Todor, O.; McCabe, R. W.; Gandhi, H. S. *Ind. Eng. Chem. Res.* **1991**, *30*, 2333.
(42) Hampson, J. A.; Rees, L. V. C. Zeolites and Microporous Crystals. In *Studies in Surface Science and Catalysis*; Hattori, T., Yashima, T., Eds.; ; Kodansha/Elsevier: Tokoy/Amserdam, 1994; pp 197−208.
(43) Rey, F., private communication.
(44) Hedin, N.; DeMartin, G. J.; Strohmaier, K. G.; Reyes, S. C. *Microporous Mesoporous Mater.* **2007**, *98*, 182.
(45) Palomino, M.; Cantín, A.; Corma, A.; Leiva, S.; Rey, F.; Valencia, S. *Chem. Commun.* **2007**, 1233.
(46) Ndjaka, J.-M. B.; Zwanenburg, G.; Smit, B.; Schenk, M. *Microporous Mesoporous Mater.* **2004**, *68*, 37.
(47) Díaz-Cabañas, M.-J.; Barrett, P. A.; Camblor, M. A. *Chem. Commun.* **1998**, 1881.
(48) Dubbeldam, D.; Smit, B. *J. Phys. Chem. B* **2003**, *107*, 12138.
(49) Dubbeldam, D.; Beerdsen, E.; Calero, S.; Smit, B. *Proc. Natl. Acad. Sci. U.S.A.* **2005**, *102*, 12317.
(50) Goj, A.; Sholl, D. S.; Akten, E. D.; Kohen, D. *J. Phys. Chem. B* **2002**, *106*, 8367.
(51) Skoulidas, A. I.; Sholl, D. S. *J. Phys. Chem. A* **2003**, *107*, 10132.
(52) Gies, H. *Z. Kristallogr.* **1986**, *175*, 93.
(53) Camblor, M. A.; Corma, A.; Lightfoot, P.; Villaescusa, L. A.; Wright, P. A. *Angew. Chem., Int. Ed.* **1997**, *36*, 2659.
(54) Vlugt, T. J. H.; Schenk, M. *J. Phys. Chem. B* **2002**, *106*, 12757.